Human Reproduction vol.15 no.5 pp.1125–1135, 2000

The effect of extracellular ice and cryoprotective agents on the water permeability parameters of human sperm plasma membrane during freezing

Ramachandra V.Devireddy[1], David J.Swanlund[1], Kenneth P.Roberts[2,3], Jon L.Pryor[2,3] and John C.Bischof[1,2,4]

[1]Bioheat and Mass Transfer Laboratory, Department of Mechanical Engineering, [2]Department of Urologic Surgery and [3]Department of Obstetrics and Gynecology, University of Minnesota, Minneapolis, MN 55455, USA

[4]To whom correspondence should be addressed

A firm biophysical basis for the cryopreservation of human spermatozoa is limited by a lack of knowledge regarding the water permeability characteristics during freezing in the presence of extracellular ice and cryoprotective agents (CPA). Cryomicroscopy cannot be used to measure dehydration during freezing in human spermatozoa because of their highly non-spherical shape and their small dimensions which are at the limits of light microscopic resolution. Using a new shape-independent differential scanning calorimeter (DSC) technique, volumetric shrinkage during freezing of human sperm cell suspensions was obtained at cooling rates of 5 and 10°C/min in the presence of extracellular ice and CPA. Using previously published data, the human sperm cell was modelled as a cylinder of length 40.2 μm and a radius of 0.42 μm with an osmotically inactive cell volume, V_b, of $0.23V_o$, where V_o is the isotonic cell volume. By fitting a model of water transport to the experimentally obtained volumetric shrinkage data, the best fit membrane permeability parameters (L_{pg} and E_{Lp}) were determined. The 'combined best fit' membrane permeability parameters at 5 and 10°C/min for human sperm cells in modified media are: $L_{pg} = 2.4 \times 10^{-14}$ m³/Ns (0.14 μm/min-atm) and $E_{Lp} = 357.7$ kJ/mol (85.5 kcal/mol) ($R^2 = 0.98$), and in CPA media (with 6% glycerol and 10% egg yolk) are $L_{pg}[cpa] = 0.67 \times 10^{-14}$ m³/Ns (0.04 μm/min-atm) and $E_{Lp}[cpa] = 138.9$ kJ/mol (33.2 kcal/mol) ($R^2 = 0.98$). These parameters are significantly different from previously published parameters for human spermatozoa obtained at suprazero temperatures and at subzero temperatures in the absence of extracellular ice. The parameters obtained in this study also suggest that damaging intracellular ice formation (IIF) could occur in human sperm cells at cooling rates as low as 25–45°C/min, depending on the concentrations of the CPA. This may help to explain the discrepancy between the empirically determined optimal cryopreservation cooling rates (<100°C/min) and the numerically predicted optimal cooling rates (>7000°C/min) obtained using previously published suprazero human sperm permeability parameters which do not account for the presence of extracellular ice.

Key words: cryopreservation/differential scanning calorimetry/human spermatozoa/membrane permeability/water transport

Introduction

From the earliest reported experiments of freezing of human spermatozoa (Spallanzani, 1776; Davenport, 1897; Parkes, 1945), there have been many improvements in the methodology of human sperm cryopreservation. Some of these improvements include the use of cryoprotectants (e.g. glycerol; Polge *et al*., 1949); the use of glycerol–egg yolk–citrate media for sperm isolation; the use of ampoules, straws and pellets; and various freezing and thawing techniques (Storey *et al*., 1998; also see review by Brotherton, 1990). In addition, several improvements have been reported on the assessment of human sperm motility, viability, energy status, damage to the plasma membrane or to the subcellular elements, chromatin stability and chromosomal damage (Watson, 1995; Royere *et al*., 1996). Both the ability to freeze and the possibility of pregnancy following intrauterine insemination (IUI) have been reported as early as 1953 (Bunge and Sherman, 1953). However, the bulk of our understanding on the effect of freezing human spermatozoa is still empirical in nature since the unique size and shape of human spermatozoa limit the applicability of traditional techniques, such as cryomicroscopy, to measure the state of intracellular water during freezing (Gao *et al*., 1997). Further improvement and increased acceptance of human sperm cryopreservation protocols necessitates a more fundamental understanding of the freezing processes in human sperm cell suspensions.

During freezing of cell suspensions, ice nucleates first in the extracellular space causing an osmotic gradient to be set up across the membrane, i.e. between the intracellular isotonic solution and the freeze-concentrated extracellular solution (Mazur, 1963). Depending on whether the cooling rate is 'low' or 'high', the intracellular water moves across the cell membrane and joins the extracellular ice phase, or freezes and forms ice inside the cell, respectively. In most cases, cells undergoing intracellular ice formation (IIF) are rendered osmotically inactive (lysed), due to the loss of cell membrane integrity (Mazur, 1984). Similarly, cells which experience a severe loss of intracellular water are also rendered osmotically inactive (Lovelock, 1953). Both IIF and long exposures to high solute concentrations are lethal to cells; thus, cooling rates which are either 'too high' or 'too low' can kill cells. Therefore, the 'optimal' cooling rate should and does exist between the 'high' and 'low' freezing rates. This has been confirmed experimentally for a variety of cells, and the curve of cell survival plotted as a function of the cooling rate has a

characteristic inverted U-shape (Mazur *et al*., 1972). Whether a prescribed cooling rate is too 'low' or too 'high', is a function of cell membrane permeability to water and the probability that any water remaining trapped within the cell at any given subzero temperature will nucleate and turn to ice. Differences in membrane permeability to water and probability of IIF result in different 'optimal' cooling rates for different cells. In general, the 'optimal' cooling rate is defined as that cooling rate which minimizes both the slow cooling and IIF injury, i.e. cool as fast as possible without forming damaging intracellular ice. Therefore, to optimize a cryopreservation protocol it is important to measure the permeability of the cell membrane to water. There are currently no experimental techniques which yield data on how sperm cells either dehydrate or form IIF during freezing in the presence of extracellular ice (Gao *et al*., 1997). Currently available cryomicroscopy techniques are limited: (i) by the resolution of the light microscope, which is close to or equal to some of the morphological dimensions of the sperm cell; and (ii) by the fact that they rely on the translation of projected two-dimensional area measurements to infer three-dimensional volumetric changes. Thus, the small radial dimensions and irregular (non-spherical) shapes of the sperm cells do not allow the observation and reduction of meaningful biophysical data through the cryomicroscope.

This study reports the use of a shape-independent differential scanning calorimeter (DSC) technique to measure the membrane permeability parameters of human sperm cells during freezing. The principle of the DSC technique can be stated as follows. During dehydration (water transport) of intact cells in the absence of intracellular freezing, the concentrations of intracellular impermeant electrolytes, substrates, cofactors, proteins, etc. increase as essentially pure water is transported across the plasma membrane into the medium where it freezes, releasing heat of fusion proportional to the amount of water removed from the cell. The cells are then lysed, and the DSC measurement then repeated exactly as before; the resulting heat released is lower because the water transport no longer functions; the difference in heat release so measured (Δq_{dsc}) is used to calculate the cell water that has permeated across the plasma membrane, from which one can deduce the cell volume (V) as a function of subzero temperature (T). The DSC technique has been applied to measure the membrane permeability parameters in a variety of biological systems, including Epstein–Barr virus transformed (EBVT) human lymphocyte cell suspensions (Devireddy *et al*., 1998), in a normal mammalian (rat) liver tissue system (Devireddy and Bischof, 1998), in Dunning AT-1 rat prostate tumour tissue (Devireddy *et al*., 1999a), in liver tissue slices of a freeze-tolerant wood frog, Rana sylvatica (Barratt *et al*., 1998; Devireddy *et al*., 1999b,c), as well as in mouse sperm cell suspensions (Devireddy *et al*., 1999d). The DSC technique is independent of the size and shape of the cells being observed, and is used in this study to measure the membrane permeability parameters of human sperm cells at two different cooling rates (5 and 10°C/min; the reasons for the choice of these cooling rates will be discussed later) in the presence of extracellular ice and cryoprotective agents (CPA). Numerical simulations of water transport in human sperm cells are then performed under a variety of cooling rates (5 to 100°C/min) using the experimentally determined membrane permeability parameters. The simulation results were analysed to predict the amount of water left in the cell after dehydration ceases, in the absence of IIF, and the 'optimal cooling rates' for human sperm cryopreservation.

Materials and methods

Mathematical modelling of water transport during freezing

In this section the mathematical equations and the membrane permeability parameters used to model water transport during freezing in the presence of extracellular ice and CPA in a cell suspension system are presented. A model has been proposed for water and solute transport in response to chemical potential gradients based on irreversible thermodynamics (Kedem and Katchalsky, 1958). The Kedem–Katchalsky model consisted of two differential equations which describe the water and CPA flux across the membrane. If the flux of CPA is negligible in comparison to the water flux (McCaa *et al*., 1991; Gilmore *et al*., 1995), then the Kedem–Katchalsky model reduces to a model which assumes only water transport, as proposed originally (Mazur, 1963) and later modified (Levin *et al*., 1976). The various assumptions made in the development of Mazur's model of water transport are discussed in detail elsewhere (McGrath, 1988). The water transport model of Mazur was further modified (Karlsson *et al*., 1993) to incorporate the presence of CPA on the volumetric shrinkage response of cells during freezing as:

$$\frac{dV}{dT} = -\frac{L_p A_c RT}{B v_w}\left[ln\frac{(V_o - V_b - n_{cpa}v_{cpa})/v_w}{(V_o - V_b - n_{cpa}v_{cpa})/v_w + (\varphi_s n_s + n_{cpa})} - \frac{\Delta H_f v_w \rho}{R}\left(\frac{1}{T_R} - \frac{1}{T}\right)\right] \quad [1]$$

with L_p, the sperm cell membrane permeability to water defined (Levin *et al*., 1976) as:

$$L_p = L_{pg}[cpa]\ exp\left(-\frac{E_{Lp}[cpa]}{R}\left(\frac{1}{T} - \frac{1}{T_R}\right)\right) \quad [2]$$

where $L_{pg}[cpa]$ is the reference membrane permeability at a reference temperature, T_R (= 273.15 K); $E_{Lp}[cpa]$ is the apparent activation energy (kJ/mol) or the temperature dependence of the cell membrane permeability; V is the sperm cell volume at a subzero temperature T (K); A_c is the effective membrane surface area for water transport, assumed to be constant during the freezing process; V_o and V_b are the isotonic (initial) and osmotically inactive sperm cell volumes respectively. In this study, the human sperm cell was modelled as a long cylinder with length (L) 40.2 μm and a radius (r_o) of 0.42 μm, which translates to V_o ~22.2 μm^3 and A_c ~106 μm^2 as reported in the literature (Curry *et al*., 1996). The value of V_b was assumed to be $0.23V_o$ (Noiles *et al*., 1993). R is the universal gas constant (8.314 J/mol K); B is the constant cooling rate (K/min); n_{cpa} is the number of moles of salt or CPA in solution; v_{cpa} is the molar volume of CPA (73.3×10^{12} μm^3/mol); v_w is the molar volume of water (18×10^{12} μm^3/mol); $[openphi]_s$ is the disassociation constant for salt (= 2); n_s is the number of moles of salt (= $C_i \bullet (V_o - V_b)$, where C_i is the initial cell osmolality, 0.285 mol/l); ΔH_f is the latent heat of fusion of water

(335 mJ/mg); ρ is the density of water (1000 kg/m^3). Note that when n_{cpa} is zero (i.e. no CPA is present), equations [1] and [2] reduce to the 'water transport' model as described earlier (Mazur, 1963; Levin *et al*., 1976), and L_p is an Arrhenius function of L_{pg} and E_{Lp}. The two unknown membrane permeability parameters of the model either $L_{pg}[cpa]$ and $E_{Lp}[cpa]$ in the presence of CPA or L_{pg} and E_{Lp} in the absence of CPA, are determined by curve-fitting the water transport model to experimentally obtained volumetric shrinkage data during freezing.

Isolation of human spermatozoa

Human semen samples were obtained from men seeking initial or follow-up evaluation for infertility at the Men's Reproductive Health Center at the University of Minnesota. Semen was collected by masturbation after 2–3 days abstinence and standard semen analyses were performed (WHO, 1999). Ejaculates with total progressive motility counts of $<10^6$ cells, or ejaculates that were positive for antisperm antibodies, were not used in this study. Additional semen samples were obtained from donors of unknown fertility status, as well as known fertile men. Within 4 h of collection, samples (usually two to four) were pooled and concentrated to 0.5–1 ml by centrifugation at 400 g for 10 min at room temperature. The concentrated sperm suspension was then re-centrifuged at 300 *g* for 25 min at room temperature through 2 ml of Isolate, a 90% density gradient medium (Irvine Scientific, Santa Ana, CA, USA), which removed most non-motile cells and seminal fluid debris. The resulting sperm pellet was resuspended to a volume of 300–500 µl in modified Biggers, Whitten and Whittingham media (modified BWW media, 282 mOsm; Irvine Scientific) and aliquots were assayed for percent viability.

Viability assay

Subsamples (~25 µl) were assayed for plasma membrane integrity by dual fluorescent dye labelling using a LIVE/DEAD Sperm Viability Kit (Molecular Probes, Eugene, OR, USA) according to the instructions provided. Briefly, SYBR-14 (live cell stain) and propidium iodide (dead cell stain) were prepared fresh daily in HEPES-buffered saline and used at final concentrations of 100 nmol/l and 600 nmol/l respectively (Garner and Johnson, 1995). Cells were first exposed to SYBR-14 for 15–30 min at 37°C followed by a 5- to 10-min incubation with propidium iodide. Between 100–300 cells from each sample were counted at 200× magnification using a BX-50 fluorescence-equipped light microscope (Olympus, Tokyo, Japan) and the appropriate filters. The mean (± SD) percentage of spermatozoa with intact plasma membranes in the pools (n = 9) was 84.0 ± 14.9.

DSC dynamic cooling experiments

For DSC experiments in the absence of CPA, sperm suspensions were concentrated a final time by centrifugation at 300 g for 5 min, resuspended to 1–200 µl in modified BWW media and placed on ice. Sperm cell concentrations were determined using a haemocytometer. All samples used in the DSC experiments had concentrations of viable cells ranging from 80×10^7 to 500×10^7 cells/ml. For DSC experiments in the presence of CPA, cells were treated in an identical manner as above except that stock CPA (48% TES–Tris, 30% citrate solution with 20% egg yolk/12% glycerol; Irvine Scientific) was added dropwise to achieve a 1:1 v/v CPA:modified BWW ratio just before the final centrifugation step (Graham *et al*., 1972; Weidel and Prins, 1987). Dropwise addition of CPA was performed to minimize osmotic injury effects (Gao *et al*., 1995; Gilmore *et al*., 1997). Thus the final concentration of CPA media was 10% egg yolk and 6% glycerol in TES–Tris–citrate solution and modified BWW media. Osmolarity of the CPA media was calculated to be 1113 mOsm,

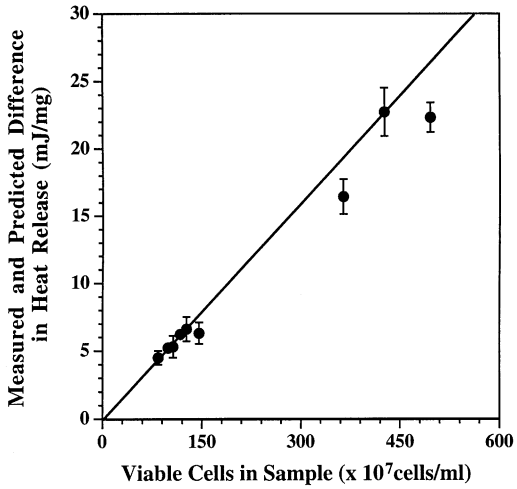

Figure 1. Plot of Δq_{dsc} as a function of initial concentration of viable cells in the differential scanning calorimeter (DSC) sample. The measured values of Δq_{dsc} are shown (•), along with the predicted value of Δq_{dsc} (——). Note that the measured values of Δq_{dsc} are in close agreement with the predicted value. The error bars represent the standard deviation in the data, i.e. the measured values of Δq_{dsc}.

which includes ~790 mOsm of glycerol. This value is supported by the osmolarity of the CPA media obtained using a vapour pressure osmometer, ~1134 ± 57 mOsm.

To ensure the accuracy and repeatability of the experimental data, the limitations of the DSC-Pyris 1 (Perkin Elmer Corporation, Norwalk, CT, USA) machine were studied, and a set of calibration and control experiments were performed as detailed previously for a DSC-7 machine (Devireddy *et al*., 1998). These included: (i) calibration and minimization of the thermal lag; (ii) baseline determination of the thermogram (a sigmoidal baseline was used); (iii) effect of *Pseudomonas syringae* on DSC heat release readings; (iv) experiments with osmotically inactive (lysed) sperm cells ($\Delta q_{dsc} = 0$); and (v) error due to noise in the DSC readings (less than 5% of Δq_{dsc}). The DSC technique presented in this study was relatively insensitive to the choice of baseline used since the heat releases were 'differences' and not 'absolute' values. In addition, the measured value of Δq_{dsc} (• in Figure 1) was shown to be proportional to the initial concentration of viable cells in the DSC sample and also agreed quite closely with the predicted value of Δq_{dsc} (—— in Figure 1).

To perform the DSC dynamic cooling experiments, the human sperm samples (7–9 mg) were placed in standard aluminium sample pans (Perkin Elmer) and a natural ice nucleator *P.syringae* (ATCC, Rockville, MD, USA) was added (0.5–1 mg) before the pans were sealed. The ice nucleating agent *P.syringae* always nucleated the extracellular space at temperatures ⩾ –5°C. The DSC pans were reweighed to measure the total sample weight (<10 mg) and the DSC experiments were performed using the dynamic cooling protocol outlined below and described in detail elsewhere (Devireddy *et al*., 1998, 1999d).

Step 1: The sample (sperm cell suspension either in modified BWW media or in the CPA media) + 0.5–1 mg of *P.syringae* bacteria initially at 4°C, was cooled at 5 (or 10) °C/min until the extracellular ice nucleated (~–3.5°C in modified BWW media and ~–4.5°C in the CPA media). Step 2: After nucleation, the sample was thawed at a warming rate (10°C/min) such that phase change temperature, T_{ph} (–0.53°C and –2.1°C for the isotonic modified BWW media and CPA media respectively) was reached (but not overshot) and ice remained in the extracellular solution. Equilibrium at T_{ph} will permit

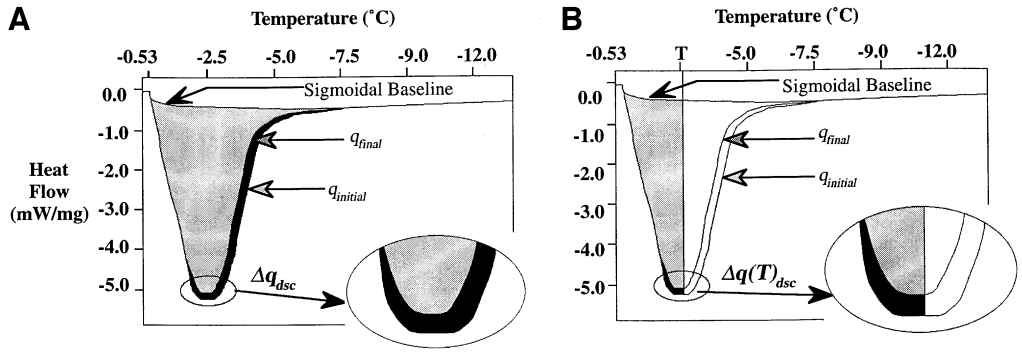

Figure 2. Superimposed heat flow thermograms obtained during the first (Step 3) and last (Step 7) of the DSC cooling protocol for human sperm cell suspension system, shown for a cooling rate of 5°C/min. The negative axis for the heat flow on the y-axis implies an exothermic heat release in the DSC sample. (**A**) Total difference between the initial (Step 3, lower curve) and the final cooling run (Step 7, upper curve) of the DSC dynamic cooling protocol. The total difference between $q_{initial}$ (Step 3) and q_{final} (Step 7) is denoted as Δq_{dsc}. (**B**) Fractional difference between the initial (Step 3, lower curve) and the final cooling run (Step 7, upper curve) of the DSC dynamic cooling protocol down to a subzero temperature, T. The fractional heat release difference between the first cooling run (Step 3), $q(T)_{initial}$, and during the last (Step 7) cooling run, $q(T)_{final}$ is denoted as $\Delta q(T)_{dsc}$.

the ice nuclei to exist but not grow into ice crystals, minimizing the osmotic shrinkage of the cells. Step 3: The sample was then cooled to –50°C at 5 (or 10) °C/min, which caused the sperm cells to undergo cellular dehydration. The lower curve in Figure 2A corresponded to the heat release associated with dehydration, and the total area is represented by $q_{initial}$. Step 4: The sample was re-equilibrated at T_{ph} by thawing at 50°C/min. Step 5: To differentiate between the heat released by the media and the intracellular fluid in Step 3, the sample was cooled at a high cooling rate (200°C/min) down to –100°C. This caused all the sperm cells to lyse and become osmotically inactive. Step 6: Step 4 was repeated. Since all the sperm cells had compromised membranes, the intracellular water, proteins and salts were now continuous (no membrane barriers existed) as previously suggested (Körber *et al*., 1991).Step 7: The sample was then cooled to –50°C at 5 (or 10) °C/min to measure the final heat release due to lysed or osmotically inactive sperm cells mixed with media. The upper curve in Figure 2A corresponded to this heat release, and the total area was represented by q_{final}.

The heat release measured during the final cooling run, q_{final} was compared with the DSC-measured heat release from a separate control experiment composed of only osmotically inactive (or lysed) human sperm cells, and the magnitude of the heat releases were found to be within ±1%. In addition, >98% of human sperm cells were found to stain with propidium iodide (dead cell stain) when the DSC pans were forced open after the fast cooling run (Step 5). This suggested that the fast cooling run in Step 5 (200°C/min to –100°C) compromised the membrane integrity of all the human sperm cells in the DSC sample.

Translation of DSC-measured heat release to dynamic cell volume data

The heat release measurements of interest were Δq_{dsc} and $\Delta q(T)_{dsc}$, which were the total and fractional differences between the heat releases measured by integration of the heat flows in Steps 3 and 7 respectively using the DSC Pyris 1 software (Perkin-Elmer Corp., Norwalk, CT, USA). The total difference in the integrated heat release between the baseline (constant and sigmoidal) and the actual thermogram in the two cooling runs (Step 3 and Step 7) was denoted as Δq_{dsc} ($= q_{initial} - q_{final}$) and is shown in Figure 2A. The fractional difference in the integrated heat release from T_{ph} down to a subzero temperature, T, is denoted by $\Delta q(T)_{dsc}$ ($= q(T)_{initial} - q(T)_{final}$) and is shown in Figure 2B. This difference in heat release has been shown to be related to cell volume changes in cell suspensions (Devireddy *et al*., 1998), in several tissue systems (Devireddy and Bischof, 1998; Devireddy *et al*., 1999a,b), and in mouse sperm cell suspensions (Devireddy *et al*., 1999d) as:

$$\frac{V_i - V(T)}{V_i - V_b} = \frac{\Delta q(T)_{dsc}}{\Delta q_{dsc}} \qquad [3]$$

This equation can be rearranged to measure water transport data from the DSC measured heat releases $\Delta q(T)_{dsc}$ and Δq_{dsc} as:

$$V(T) = V_i - \frac{\Delta q(T)_{dsc}}{\Delta q_{dsc}} \bullet (V_i - V_b). \qquad [4]$$

Note that the DSC-measured heat release readings $\Delta q(T)_{dsc}$ and Δq_{dsc} are obtained separately at 5°C/min (shown in Figure 2 for sperm cells suspended in modified BWW media) and at 10°C/min (data not shown) both in the absence and presence of CPA. The DSC water transport data obtained using equation [4] were shown to generate statistically similar data [statistically insignificant differences ($P > 0.05$) by Student's *t*-test] to those obtained using a standard cellular cryomicroscopy technique with a spherical cell system (Devireddy *et al*., 1998), and also to the water transport data obtained using the low-temperature microscopy method in a normal rat liver tissue system (Devireddy and Bischof, 1998). Since the use of equation [4] to generate water transport data from DSC-measured heat release readings has been validated in both cell and tissue systems, it is reasonable to presume that it can also be used to generate the water transport data in a sperm cell suspension system. The unknowns needed in equation [4], apart from the DSC heat release readings, are V_i (the initial cell volume) and V_b (the osmotically inactive cell volume). The initial volume of the sperm cells in both modified BWW media and the CPA media was assumed to be the isotonic cell volume, V_o (~22.2 μm^3) as reported earlier (Curry *et al*., 1996). As stated above, the osmotically inactive cell volume, V_b, was assumed to be $0.23V_o$ in modified BWW media, while in the CPA media the presence of glycerol in the intracellular compartment increased the osmotically inactive cell volume to ~$0.32V_o$.

Numerical methods

A non-linear least squares curve fitting technique was implemented using a computer program to calculate the membrane permeability parameters (L_{pg} and E_{Lp}) that best fit the volumetric shrinkage data

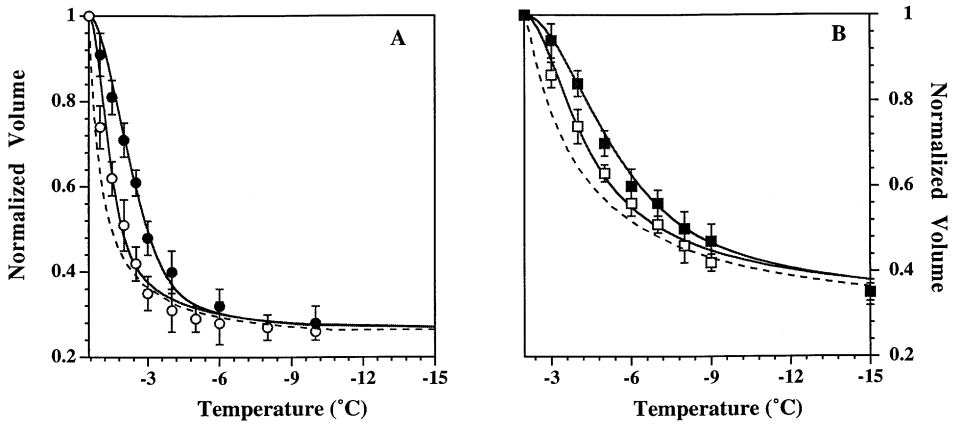

Figure 3. Volumetric response of human spermatozoa as a function of subzero temperatures obtained using the DSC technique in (**A**) modified BWW media and (**B**) CPA media. The open (○,□) and closed (●,■) symbols represent the 5 and 10°C/min data respectively. The model simulated equilibrium cooling response is shown as a dotted line in both figures. The model simulated dynamic cooling response at 5 and 10°C/min is shown as a solid line and was obtained by using the 'best fit' membrane permeability parameters (L_{pg} and E_{Lp} or $L_{pg}[cpa]$ and $E_{Lp}[cpa]$) shown in Table I, in the water transport equation (equations [1] and [2]).

as previously described (Bevington and Robinson, 1992). The optimal fit of equation [1] to the experimental data was obtained by selecting a set of parameters which minimized the residual variance, χ^2, and maximized a goodness of fit parameter, R^2 (Montgomery and Runger, 1994). In order to predict the membrane permeability parameters that produced a 'combined best fit' to the experimental water transport data at two or more cooling rates, the non-linear curve fitting code was slightly modified such that R^2 was minimized by one set of parameters for all cooling rates as described previously (Smith *et al*., 1998). All the curve fitting results presented have an R^2 value greater than or equal to 0.97, indicating that there was a good agreement between the experimental data points and the fit calculated using the estimated membrane permeability parameters. To simulate the biophysical response of a sperm cell under a variety of cooling rates the best fit parameters were substituted in the water transport equation (equations [1] and [2]), which was then numerically solved using a fourth-order Runge–Kutta method using a FORTRAN code on a SGI (SGI, Mountain View, CA, USA) workstation (Pazhayannur and Bischof, 1997).

Results

Dynamic cooling response and membrane permeability parameters

Water transport data and simulation using best fit parameters in equation [1] at cooling rates of 5 and 10°C/min in modified BWW media are shown in Figure 3A. The dynamic portion of the cooling curve was between –0.53°C and –10°C at these cooling rates. Water transport cessation was observed in the DSC heat release data as an overlap of the thermograms from the first (Step 3) and last (Step 7) run, as seen in Figure 2. The best fit of equation [1] to the 5°C/min water transport data was obtained for membrane permeability parameter values of $L_{pg} = 3.7\times10^{-14}$ m^3/Ns (0.22 μm/min-atm) and E_{Lp} = 391.2 kJ/mol (93.5 kcal/mol) with an R^2 value of 0.99, while the corresponding values for the 10°C/min data were $L_{pg} = 1.9\times10^{-14}$ m^3/Ns (0.11 μm/min-atm) and E_{Lp} = 312.5 kJ/mol (74.7 kcal/mol) with an R^2 value of 0.99 (Table I). The model simulated equilibrium cooling response [equilibrium was achieved at each temperature when the internal and external osmotic pressures were equal (i.e. $\pi_i = \pi_o$)] was generated by setting the left-hand side of equation [1] = 0 and balancing the intracellular and extracellular unfrozen chemical activity of water on the right-hand side at a particular subzero temperature.

Water transport data and simulation using best fit parameters in equation [1] at cooling rates of 5 and 10°C/min in the CPA media (as described earlier) are shown in Figure 3B. The dynamic portion of the cooling curve was between –0.53°C and –15°C at these cooling rates. The best fit of equation [1] to the 5°C/min water transport data was obtained for membrane permeability parameter values of $L_{pg}[cpa] = 1.01\times10^{-14}$ m^3/Ns (0.06 μm/min-atm) and $E_{Lp}[cpa]$ = 194.6 kJ/mol (46.5 kcal/mol) with an R^2 value of 0.99, while the corresponding values for the 10°C/min data were $L_{pg}[cpa] = 0.67\times10^{-14}$ m^3/Ns (0.04 μm/min-atm) and $E_{Lp}[cpa]$ = 131.8 kJ/mol (31.5 kcal/mol) with an R^2 value of 0.99 (Table I).

Statistical analysis

The differences in the water transport data between the 5 and 10°C/min rates shown in Figure 3A and B were not statistically significant. However, the differences between the data obtained in the presence and absence of CPA were statistically significant in the dynamic part of the cooling curve (>80% confidence level using Student's *t*-test). The 10°C/min dynamic data were statistically significant from the equilibrium cooling response, both in the presence and absence of CPA (with >90% confidence level). However, the differences between the 5°C/min data and the equilibrium cooling response were not statistically significant.

Combined best fit parameters

A new set of membrane permeability parameters (L_{pg} and E_{Lp} or $L_{pg}[cpa]$ and $E_{Lp}[cpa]$) were obtained that produced a 'combined best fit' to the experimentally determined water

Table I. Predicted subzero membrane permeability parameters for human sperm cells in the presence of extracellular ice and cryoprotective agents (CPA), assuming $V_b = 0.23V_o$

Experimental media	Cooling rate (°C/min)	L_{pg} or $L_{pg}[cpa]$ $\times 10^{14}$ m^3/Ns (μm/min-atm)	E_{Lp} or $E_{Lp}[cpa]$ kJ/mol (kcal/mol)	R^2 value
Buffer solution[a]	5	3.7 (0.22)	391.2 (93.5)	0.99
	10	1.9 (0.11)	312.5 (74.7)	0.99
	Combined best fit[c1]	2.4 (0.14)	357.7 (85.5)	0.98
CPA media[b]	5	1.01 (0.06)	194.6 (46.5)	0.99
	10	0.67 (0.04)	131.8 (31.5)	0.99
	Combined best fit[c]	0.67 (0.04)	138.9 (33.2)	0.98

[a]Modified Biggers, Whitten and Whittingham (BWW) media.
[b]6% glycerol and 10% egg yolk in buffer solution.
[c]The combined best fit parameters minimized the R^2 value, concurrently, at both 5 and 10°C/min.

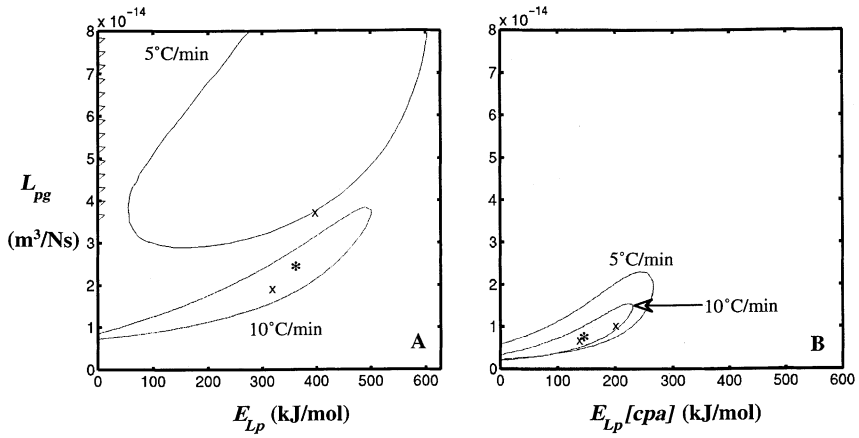

Figure 4. Contour plots of the goodness of fit parameter R^2 (= 0.98) for water transport response in human spermatozoa in (**A**) modified BWW media and (**B**) CPA media. The common region corresponds to the range of parameters that 'fit' the water transport data at both the cooling rate (either 5 or 10°C/min) with $R^2 \geq 0.98$. Note that the 'combined best fit' parameters are represented by '*' in both the figures, while the 'x' represent the 'best fit' parameters at either 5 or 10°C/min.

transport data in modified BWW media and in the CPA media, as shown in Table I. The 'combined best fit' membrane permeability parameters maximized the goodness of fit parameter, R^2, for the 5 and 10°C/min water transport data concurrently. The contour plots of the goodness of fit parameter, R^2 (= 0.98) in the L_{pg} and E_{Lp} (or $L_{pg}[cpa]$ and $E_{Lp}[cpa]$) space that 'fit' the water transport data at 5 and 10°C/min in modified BWW media and in the CPA media, are shown in Figure 4A and B respectively. Any combination of L_{pg} and E_{Lp} (or $L_{pg}[cpa]$ and $E_{Lp}[cpa]$) shown to be within the contour will 'fit' the water transport data at that cooling rate, with an R^2 value >0.98. An interesting observation was the 'serrations' on the y-axis in Figure 4A, which corresponded to the contour space that fitted the water transport data at 5°C/min. These 'serrations' showed that combinations of E_{Lp} ~0.0 and L_{pg} ranging from 3.5 to 8×10^{-14} m^3/Ns (~0.2 to 0.5 μm/min-atm) can also simulate the 5°C/min data in the absence of CPA with a goodness of fit parameter, R^2 >0.98. Note that the contour space that fitted the water transport data in the presence of CPA (Figure 4B) was significantly smaller than in the absence of CPA (Figure 4A), suggesting that a smaller set of parameters could predict the water transport response in the presence of CPA.

In Figure 4A and B, the 'combined best fit' parameters compared quite closely with the parameters obtained at the higher cooling rate of 10°C/min, presumably due to the fact that the 10°C/min water transport data were farther away from equilibrium than the 5°C/min data. This suggested that the membrane permeability parameters obtained using the 10°C/min water transport data could predict the volumetric response of the sperm cell at the lower cooling rate of 5°C/min quite accurately, while the converse was not true. This suggestion was clearly supported by the contours shown in Figure 4B, where the contour for 10°C/min data was almost completely enclosed by the contour for 5°C/min. Therefore, in order to obtain the membrane permeability parameters that 'best predict' the behaviour of a biological system, water transport data need to be obtained at the highest possible cooling rate at which dehydration occurs exclusively, as noted earlier (Smith *et al.*, 1998; Devireddy *et al.*, 1999a,d).

Simulations of water transport

Water transport simulations obtained using the 'combined best fit' parameters in equation [1] are shown for a variety of cooling rates (5–100°C/min) in Figure 5. In Figure 5A and B, the numerically simulated non-dimensional cellular volume

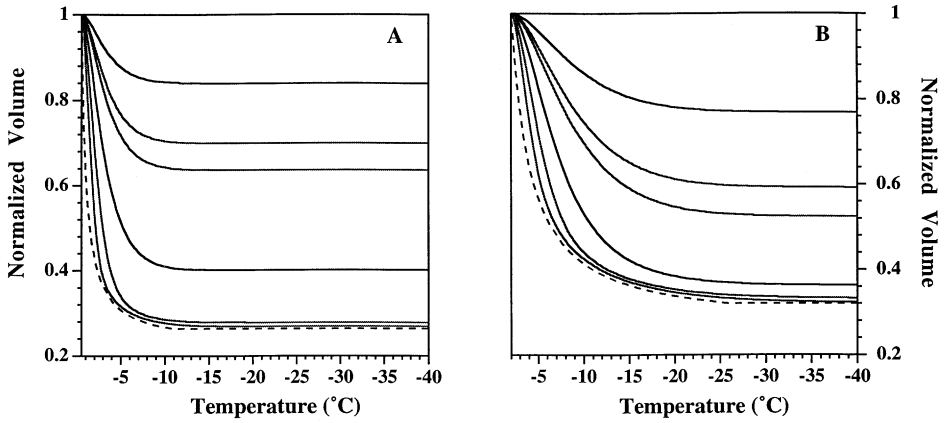

Figure 5. Volumetric response of human spermatozoa at various cooling rates as a function of subzero temperatures using the 'combined best fit' membrane permeability parameters (shown in Table I) in (**A**) modified BWW media and (**B**) CPA media. The water transport curves (solid lines) represent the model simulated response for different cooling rates (from left to right: 5, 10, 20, 40, 50 and 100°C/min). The model simulated equilibrium cooling response is also shown in both figures as a dotted line.

(V/V_o) obtained using these 'combined best fit' parameters is shown for a variety of cooling rates (at 5, 10, 20, 40, 50 and 100°C/min) in modified BWW media and in the CPA media respectively. The non-dimensional cellular volume (V/V_o), which decreased due to dehydration during freezing, was plotted on the y-axis, while the subzero temperatures were plotted on the x-axis. From the simulations, the amount of trapped water (or a lower bound on the intracellular ice) was computed as a ratio of the volume of the water trapped inside the sperm cell at the temperature, T (~–30°C) where intracellular ice formation can occur by a homogeneous or volume-catalysed nucleation (Toner, 1993) to the initial sperm water volume, $[(V–V_b)/(V_o–V_b)]$ as described earlier for a rat liver tissue system (Pazhayannur and Bischof, 1997). Note that V was the end volume after water transport ceased (at ~–30°C), and V_o and V_b were the initial (isotonic) and final (osmotically inactive) sperm cell volumes respectively. In modified BWW media, for cooling rates of ⩽10, 20, 40, 50 and 100°C/min, the trapped water volume was ⩽1.2, 22.2, 52.7, 60.1 and 79.1% of initial osmotically active water volume respectively, and the corresponding end volumes were $\leqslant 0.24V_o$, $0.4V_o$, $0.64V_o$, $0.7V_o$ and $0.84V_o$ respectively (Figure 5A). In the CPA media (Figure 5B), for cooling rates of ⩽10, 20, 40, 50 and 100°C/min, the trapped water volume was ⩽2.4, 6.7, 30.2, 40.3 and 66.2% of initial osmotically active water volume respectively. Therefore, depending on the concentrations of the CPA, the water transport simulations (Figure 5) showed that cooling rates as low as 20°C/min could cause intracellular water to be trapped within the human sperm cells. With sufficient supercooling, this trapped water would ultimately form intracellular ice.

As described earlier (see Introduction), the cooling rate which optimizes the freeze–thaw response of any cellular system can be defined as the fastest cooling rate in a given media without forming damaging IIF (Mazur *et al*., 1972). IIF was defined as damaging and lethal for embryos if >10–15% of the initial intracellular water was involved (Mazur, 1990). We defined the 'optimal cooling rate' as the cooling rate at which ~5% of the initial osmotically active water volume was trapped inside the cells at temperature, T ~–30°C. The simulations (shown in Figure 5) showed that the 'optimal cooling rate' in modified BWW media and in the CPA media were ~14 and ~16°C/min respectively. Note, that if IIF occurred by a heterogeneous or a surface-catalysed nucleation mechanism (Toner, 1993) (generally between –5 and –20°C for a variety of single cells)–which our model does not predict–then potentially even more water would be trapped in the sperm cells than predicted by water transport alone (i.e. the lower bound of intracellular ice discussed above). Thus, the 'optimal cooling rates' (stated above) based on the lower bound of intracellular ice are probably an overestimation.

Discussion

Parameter sensitivity analysis: effect of varying the osmotically inactive cell volume (V_b)

The value of the osmotically inactive cell volume of human sperm cells has been reported to range from $0.23V_o$ (the value used in this study; Noiles *et al*., 1993) to ~$0.5V_o$ (Gilmore *et al*., 1995). To study the effect of varying the osmotically inactive cell volume on the predicted membrane permeability parameters (L_{pg} and E_{Lp}), the value of V_b was changed to $0.5V_o$. The DSC data were correspondingly modified (using equation [4]) and the modified DSC water transport data were curve-fitted to the water transport model (equations [1] and [2]) using the non-linear least squares curve fitting technique as described previously. The predicted values of the membrane permeability parameters (L_{pg} and E_{Lp}), using a value of $V_b = 0.5V_o$, are shown in Table II. An increase of ~117% in the value of V_b from $0.23V_o$ to $0.5V_o$ resulted in the model-predicted membrane permeability parameters being within 30% of the each other (as shown in Tables I and II). This lack of sensitivity in the membrane permeability parameters to the value of the osmotically inactive cell volume has been reported in the literature for a variety of cell and tissue systems (Pazhayannur and Bischof, 1997; Devireddy *et al*., 1998, 1999a). Thus, errors in the estimated value of V_b can alter the

Table II. Predicted sub-zero membrane permeability parameters for human sperm cells in the presence of extracellular ice and cryoprotective agents (CPA), assuming $V_b = 0.5V_o$

Experimental media	Cooling rate (°C/min)	L_{pg} or $L_{pg}[cpa]$ $\times 10^{14}$ m^3/Ns (μm/min-atm)	E_{Lp} or $E_{Lp}[cpa]$ kJ/mol (kcal/mol)	R^2 value
Buffer solution[a]	5	2.7 (0.16)	487.8 (116.6)	0.98
	10	1.5 (0.09)	384.0 (91.8)	0.98
	Combined best fit[c]	1.8 (0.11)	431.7 (103.2)	0.97
CPA media[b]	5	0.83 (0.05)	202.3 (48.4)	0.98
	10	0.50 (0.03)	139.2 (33.3)	0.97
	Combined best fit[c]	0.50 (0.03)	144.6 (34.6)	0.97

[a]Modified Biggers, Whitten and Whittingham (BWW) media.
[b]6% glycerol and 10% egg yolk in buffer solution.
[c]The combined best fit parameters minimized the R^2 value, concurrently, at both 5 and 10°C/min.

model predicted membrane permeability parameters (L_{pg} and E_{Lp}), but the trends remain the same.

The effect of varying the osmotically inactive cell volume on the model-simulated value of trapped water (or a lower bound on intracellular ice) was also investigated. This was done by performing additional water transport simulations using the 'combined best fit' parameters shown in Table II. When the value of V_b was assumed to be $0.5V_o$, in modified BWW media, for cooling rates of ⩽10, 20, 40, 50 and 100°C/min, the trapped water volume was ⩽1.9, 28.2, 56.5, 66.4 and 82.3% of initial osmotically active cell volume respectively. The corresponding values in the CPA media were ⩽2.1, 9.2, 29.2, 41.3 and 65.1% of initial osmotically active cell volume respectively. These values were comparable with those obtained earlier using a V_b value of $0.23V_o$. Thus, the variation in the value of V_b does not significantly alter the model predictions and, as noted earlier depending on the concentration of CPA, cooling rates as low as 20°C/min can cause significant amounts of intracellular water to be trapped inside human spermatozoa.

Experiments at higher cooling rates

As noted earlier and in other studies, it is essential that water transport parameters be obtained at the highest possible cooling rate at which dehydration occurs exclusively (Smith *et al*., 1998; Devireddy *et al*., 1999a,d). One of the main disadvantages of the DSC technique is that it cannot distinguish between the heat releases obtained during water transport and IIF. So, a correlative method is needed to determine that the biophysical response is in fact water transport and not IIF (Devireddy and Bischof, 1998; Devireddy *et al*., 1998). Since standard cellular cryomicroscopy cannot be used to determine the biophysical response during freezing in human spermatozoa, an indirect methodology was used to determine the maximum cooling rate at which water transport occurred exclusively in human spermatozoa. It has been reported (Henry *et al*., 1993) that the plot of motility, plasma membrane integrity and mitochondrial function versus cooling rate resembles an inverted 'U' curve with an optimal cooling rate of 10°C/min (with rapid thawing rate) in the presence of 0.85 mol/l glycerol. These data suggest that the loss of motility, plasma membrane integrity and mitochondrial function at cooling rates >10°C/min are due to the formation of IIF. Thus, the highest cooling rate which causes water transport to occur exclusively in human spermatozoa in the presence of 0.85 mol/l glycerol (which is very close to the concentration of glycerol used in this study, 0.79 mol/l) is ~10°C/min, and hence DSC experiments were not performed at higher cooling rates. It is possible that in the absence of CPA, some IIF may occur at 10°C/min. However, for the purpose of this study this possibility was considered negligible.

Membrane transport parameters in the absence of extracellular ice

As mentioned earlier, there are currently no experimental techniques which yield data on how sperm cells either dehydrate or form intracellular ice during freezing in the presence of extracellular ice (Gao *et al*., 1997). However, there exist a few techniques such as the 'time to lysis' method (Noiles *et al*., 1993; Watson, 1995) and the 'Coulter counter' technique (Gilmore *et al*., 1995) to measure the volumetric response of sperm cells to external changes in osmolarity at suprazero temperatures. The parameters obtained using these techniques, suprazero membrane permeability, L_p ~0.85–5.1×10^{-13} m^3/Ns (0.5–3 μm/min-atm) and activation energy at suprazero temperatures, E_a ~12–30 kJ/mol (3–7 kcal/mol), serve to provide a good understanding of suprazero water transport response for human sperm cells (Gao *et al*., 1997). The suprazero membrane permeability, L_p of human sperm cells is higher than that of other mammalian cells [with the possible exception of red blood cells (RBC) and hepatocytes] and activation energies, E_a are low in comparison with other mammalian cells (Curry *et al*., 1994; Gao *et al*., 1997). One reason for the high permeability values might be the presence of channel-forming proteins selective to water in the sperm plasma cell membrane. For example, the high membrane permeability value reported for human RBC is due to the presence of CHIP28, a channel-forming protein. It has been shown (Liu *et al*., 1995) that CHIP28 does not mediate the water transport process in human sperm cells. However, the presence of an analogue to CHIP28 in the sperm cell plasma membrane cannot be ruled out (Hasegawa *et al*., 1994; Gilmore *et al*., 1995). It should also be noted that water-transporting proteins (water channels, aquaporins) were identified in several

parts of the reproductive system, including the testis efferent ductules, seminal vesicles, prostate, uterus and placenta (see review by Verkman *et al*., 1996).

Suprazero permeability parameters cannot predict subzero response

The extrapolation of the suprazero permeability data obtained in the absence of extracellular ice using the techniques described above to subzero temperatures in the presence of extracellular ice has not been successful (Curry *et al*., 1994). This conclusion is based on the fact that water permeabilities predicted on the basis of the above-mentioned techniques suggest that human sperm cells should be able to dehydrate at cooling rates up to 7000°C/min during freezing, when in fact experiments show that the 'optimal cooling rate' for human sperm cells is <100°C/min depending on the concentrations of CPA in the extracellular milieu (Henry *et al*., 1993; Curry *et al*., 1994). One reason for this discrepancy may be that the values of membrane permeability parameters at subzero temperatures in the presence of extracellular ice are markedly different than those reported in the literature at suprazero temperatures. In particular, if L_{pg} at subzero temperatures is lower by at least an order of magnitude than L_p at suprazero temperatures, and E_{Lp} at subzero temperatures is higher by at least an order of magnitude than the corresponding E_a at suprazero temperatures, then the discrepancy between numerical simulations and experimental data can be reconciled (Gao *et al*., 1997). The best fit parameters obtained in this study using the DSC water transport data (shown in Tables I and II) during freezing of human spermatozoa, confirm that this is indeed the case; L_{pg} ~3.7–0.5×10^{-14} m^3/Ns (0.22–0.03 μm/min-atm) and E_{Lp} ~130–503 kJ/mol (31–120 kcal/mol).

The discrepancy between the membrane permeabilities determined in this study and the suprazero permeabilities reported in previous studies may be associated with possible changes in the sperm cell plasma membrane during cooling. These changes could include either a lipid phase transition between 0 and 4°C and/or a cold shock damage or 'chilling' injury during cooling (Watson, 1981; Drobnis *et al*., 1993). The presence of extracellular ice further alters the cell membrane transport properties, as measured using cryomicroscopy for a variety of cells. In general, for mammalian cells the average activation energy obtained in the presence of extracellular ice is approximately twice as large as that for studies conducted in unfrozen solutions at higher temperatures (McGrath, 1988). It has been found that for human granulocytes the activation energy is dramatically higher (~3 times) and membrane permeability is dramatically lower (~10–15 times) at subzero temperatures in the presence of extracellular ice, when compared with activation energy at suprazero temperatures in the absence of extracellular ice (Schwartz and Diller, 1983). This trend is consistent with the results obtained in this study for human sperm cells and in a previous study of mouse sperm cells (Devireddy *et al*., 1999d). These changes in membrane transport properties at lower temperatures might be associated with a variety of thermotropic (temperature-dependent) phase phenomena. For example, the temperature reduction which induces solidification in the extracellular medium may lead to lyotropic (i.e. independent of cooling rate) membrane phase changes and corresponding alterations of membrane permeability (Steponkus, 1984; Caffrey, 1987). The relative importance of temperature and the effect of extracellular ice on the membrane permeability L_p, is dependent on the cell type. The present study shows that human sperm cells have dramatically different membrane permeabilities at subzero temperatures in the presence of extracellular ice as compared with previously published values at suprazero temperatures.

Membrane transport parameters in the presence of CPA

The DSC technique was used to obtain water transport data and water permeability parameters ($L_{pg}[cpa]$ and $E_{Lp}[cpa]$) of human sperm cells in the presence of extracellular ice and CPA. Although the exact mechanism by which the presence of CPA modifies the water permeability parameters is as yet unknown, several studies have shown that the presence of CPA tends to reduce the membrane permeability parameters, $L_{pg}[cpa]$ and $E_{Lp}[cpa]$. A similar trend is seen in the data shown in Tables I and II, where an increase in the concentration of solutes in the extracellular medium is shown to decrease the predicted value of reference membrane permeability of human sperm cells, L_{pg} from 2.4×10^{-14} m^3/Ns (0.14 μm/min-atm) in modified BWW media to $L_{pg}[cpa]$ of 0.67×10^{-14} m^3/Ns (0.04 μm/min-atm) in CPA media. This trend is consistent with results reported in previous studies on membrane permeability parameters of ova and embryos (Mazur, 1990). It was demonstrated that the value of $L_p[cpa]$ obtained in the presence of various CPA [1 mol/l glycerol; 1 mol/l propylene glycol; 1 mol/l dimethylsulphoxide (DMSO) and 2 mol/l ethylene glycol] was lower by 30–60% than that obtained in their absence for human sperm cells at suprazero temperatures (i.e. $L_p[cpa] < L_p$) (Gilmore *et al*., 1995). A similar decrease was also reported in the value $L_{pg}[cpa]$ in isolated rat hepatocytes in the presence of 1 mol/l and 2 mol/l DMSO using standard cellular cryomicroscopy (Smith *et al*., 1998). Earlier, it was stated (Mazur, 1990) that E_{Lp} remains unaltered due to changes in the extracellular concentration (i.e. $E_{Lp}[cpa] \sim E_{Lp}$), while others (Gilmore *et al*., 1995) measured an increase (by a factor of 2 to 3) in the value of the $E_a[cpa]$ for human sperm cells (i.e. $E_a[cpa] > E_a$) using a Coulter counter technique. A reduction (by ~40–60%) was also found in the value of $E_{Lp}[cpa]$ with increasing concentrations of DMSO for isolated rat hepatocytes (i.e. $E_{Lp}[cpa] < E_{Lp}$) (Smith *et al*., 1998).

To conclude, a new shape-independent differential scanning calorimeter (DSC) technique was used in this study to obtain the volumetric shrinkage during freezing of human sperm cell suspensions in the presence of extracellular ice and CPA at two different cooling rates (5 and 10°C/min). By fitting a model of water transport to the experimentally obtained volumetric shrinkage data, the best fit membrane permeability parameters (L_{pg} and E_{Lp}) were determined. The parameters obtained in this study (L_{pg} ~0.22 to 0.03 μm/min-atm and E_{Lp} ~30 to 120 kcal/mol, with and without the presence of CPA respectively) were significantly different from the membrane permeability parameters reported in the literature for human spermatozoa in the absence of extracellular ice at suprazero

(and subzero) temperatures (L_p ~0.5–3.0 μm/min-atm and E_a ~3.0–7.0 kcal/mol, with and without the presence of CPA respectively). The new parameters obtained in this study help to explain the discrepancy in the predicted optimal cooling rates based on suprazero permeability parameters (~7000°C/min) and the experimentally determined optimal cooling rates (<100°C/min). It is hoped that the experimentally determined water transport data and modelling made available by the new DSC technique will lead to an understanding of how to optimize human sperm cryopreservation protocols on a firm biophysical basis.

Acknowledgements

This work was supported by NSF-BES # 9703326 and a grant from Reproductive Health Associates (RHA), St Paul, Minnesota, USA.

References

Barratt, P.R., Devireddy, R.V., Storey, K.B. and Bischof, J.C. (1998) Biophysics of freezing in liver of the freeze-tolerant wood frog R. sylvatica. *Ann. N. Y. Acad. Sci.*, **858**, 284–297.

Bevington, P.R. and Robinson, D.K. (1992) Data Reduction and Error Analysis for the Physical Sciences, 2nd edn. McGraw-Hill, New York.

Brotherton, J. (1990) Cryopreservation of human sperm. *Arch. Andr.*, **25**, 181–195.

Bunge, R.G. and Sherman, J.K. (1953) Fertilizing capacity of frozen human spermatozoa. *Nature*, **172**, 767.

Caffrey, M. (1987) The combined and separate effects of low temperature and freezing on membrane lipid mesomorphic phase behavior: relevance to cryobiology. *Biochim. Biophys. Acta*, **896**, 123–127.

Curry, M.R., Millar, J.D. and Watson, P.F. (1994) Calculated optimal cooling rates for ram and human sperm cryopreservation fail to conform with empirical observations. *Biol. Reprod.*, **51**, 1014–1021.

Curry, M.R., Millar, J.D., Tamuli, S.M. and Watson, P.F. (1996) Surface area and volume measurements for ram and human spermatozoa. *Biol. Reprod.*, **55**, 1325–1332.

Davenport, C.B. (1897) Experimental Morphology: Part I, Effect of Chemical and Physical Agents upon Protoplasm. Macmillan Company, New York.

Devireddy, R.V. and Bischof, J.C. (1998) Measurement of water transport during freezing in mammalian liver tissue – Part II: The use of differential scanning calorimetry. *ASME J. Biomech. Eng.*, **120**, 559–569.

Devireddy, R.V., Raha, D. and Bischof, J.C. (1998) Measurement of water transport during freezing in cell suspensions using a differential scanning calorimeter. *Cryobiology*, **36**, 124–155.

Devireddy, R.V., Smith, D.J. and Bischof, J.C. (1999a) Mass transfer during freezing in rat prostate tumor tissue. *AIChE J.*, **45**, 639–654.

Devireddy, R.V., Barratt, P.R., Storey, K.B. and Bischof, J.C. (1999b) Liver freezing response of the freeze tolerant wood frog, Rana sylvatica, in the presence and absence of glucose. I. Experimental measurements. *Cryobiology*, **38**, 310–326.

Devireddy, R.V., Barratt, P.R., Storey, K.B. and Bischof, J.C. (1999c) Liver freezing response of the freeze tolerant wood frog, Rana sylvatica, in the presence and absence of glucose. II. Mathematical modeling. *Cryobiology*, **38**, 327–338.

Devireddy, R.V., Swanlund, D.J., Roberts, K.P. and Bischof, J.C. (1999d) Sub-zero water permeability parameters of mouse spermatozoa in the presence of extracellular ice and cryoprotective agents. *Biol. Reprod.*, **61**, 764–775.

Drobnis, E.Z., Crowe, L.M., Berger, T. *et al*. (1993) Cold shock damage is due to lipid phase transitions in cell membranes: a demonstration using sperm as a model. *J. Exp. Zool.*, **265**, 432–437.

Gao, D.Y., Liu, J., Liu, C. *et al*. (1995) Prevention of osmotic injury to human spermatozoa during addition and removal of glycerol. *Hum. Reprod.*, **10**, 1109–1122.

Gao, D.Y., Mazur, P. and Critser, J.K. (1997) Fundamental cryobiology of mammalian spermatozoa. In Karow, A.M. and Critser, J.K. (eds), *Reproductive Tissue Banking*, Academic Press, San Diego, CA, pp. 263–328.

Garner, G.L. and Johnson, L.A. (1995) Viability assessment of mammalian sperm using SYBR-14 and propidium iodide. *Biol. Reprod.*, **53**, 276–284.

Gilmore, J.A., McGann, L.E., Liu, J. *et al*. (1995) Effect of cryoprotectant solutes on water permeability of human spermatozoa. *Biol. Reprod.*, **53**, 985–995.

Gilmore, J.A., Liu, J., Gao, D.Y. and Critser, J.K. (1997) Determination of optimal cryoprotectants and procedures for their addition and removal from human spermatozoa. *Hum. Reprod.*, **12**, 112–118.

Graham, E.F., Crabo, B.G. and Brown, K.I. (1972) Effects of some zwitter ion buffers on the freezing and storage of spermatozoa. I. Bull. *J. Dairy Sci.*, **55**, 372–378.

Hasegawa, H., Ma, T., Skach, W. *et al*. (1994) Molecular cloning of mercurial-insensitive water channel expressed in selected water-transporting tissues. *J. Biol. Chem.*, **269**, 5497–5500.

Henry, M.A., Noiles, E.E., Gao, D. *et al*. (1993) Cryopreservation of human spermatozoa. IV. The effects of cooling rate and warming rate on the maintenance of motility, plasma membrane integrity, and mitochondrial function. *Fertil. Steril.*, **60**, 911–918.

Karlsson, J.O., Cravalho, E.G., Borel, R.I. *et al*. (1993) Nucleation and growth of ice crystals inside cultured hepatocytes during freezing in the presence of dimethylsulfoxide. *Biophys. J.*, **65**, 2524–2536.

Kedem, O. and Katchalsky, A. (1958) Thermodynamic analysis of the permeability of biological membranes to non-electrolytes. *Biochim. Biophys. Acta*, **27**, 229–246.

Körber, C.H., Englich, S. and Rau, G. (1991) Intracellular ice formation: cryomicroscopical observation and calorimetric measurement. *J. Microsc.*, **161**, 313–325.

Levin, R.L., Cravalho, E.G. and Huggins, C.G. (1976) A membrane model describing the effect of temperature on the water conductivity of erythrocyte membranes at subzero temperatures. *Cryobiology*, **13**, 415–429.

Liu, C., Gao, D., Preston, G. *et al*. (1995) High water permeability of human spermatozoa is mercury resistant and not mediated by CHIP28. *Biol. Reprod.,* **52**, 913–919.

Lovelock, J.E. (1953) Haemolysis of human red blood-cells by freezing and thawing. *Biochim. Biophys. Acta*, **10**, 414–426.

Mazur, P. (1963) Kinetics of water loss from cells at subzero temperatures and the likelihood of intracellular freezing. *J. Gen. Physiol.*, **47**, 347–369.

Mazur, P. (1984) Freezing of living cells: mechanisms and implications. *Am. J. Physiol.*, **247**, C125–C142.

Mazur, P. (1990) Equilibrium, quasi-equilibrium, and nonequilibrium freezing of mammalian embryos (review). *Cell Biophys.*, **17**, 53–92.

Mazur, P., Leibo, S.P. and Chu, E.H.Y. (1972) A two-factor hypothesis of freezing injury. *Exp. Cell Res.*, **71**, 345–355.

McCaa, C., Diller, K.R., Aggarawal, S.J. and Takahashi, T. (1991) Cryomicroscopic determination of the membrane osmotic properties of human monocytes at subfreezing temperatures. *Cryobiology*, **28**, 391–399.

McGrath, J.J. (1988) Membrane transport properties. In McGrath, J.J. and Diller, K.R. (eds), *Low Temperature Biotechnology: Emerging Applications and Engineering Contributions*. *BED*-Vol. **10**, *HTD*-Vol. **98**, ASME Press, pp. 273–330.

Montgomery, D.C. and Runger, G.C. (1994) Applied Statistics and Probability for Engineers. John Wiley & Sons, Inc., New York, pp. 471–529.

Noiles, E.E., Mazur, P., Watson, P.F. *et al*. (1993) Determination of water permeability coefficient for human spermatozoa and its activation energy. *Biol. Reprod.*, **48**, 99–109.

Parkes, A.S. (1945) Preservation of human spermatozoa at low temperatures. *Br. Med. J.*, **ii**, 212–213.

Pazhayannur, P.V. and Bischof, J.C. (1997) Measurement and simulation of water transport during freezing in mammalian liver tissue. *ASME J. Biomech. Eng.*, **119**, 269–277.

Polge, C., Smith, A.U. and Parkes, A.S. (1949) Revival of spermatozoa after vitrification and dehydration at low temperatures. Nature, **164**, 666.

Royere, D., Barthelemy, C., Hamamah, S. and Lansac, J. (1996) Cryo-preservation of spermatozoa: a 1996 review. *Hum. Reprod. Update*, **2**, 553–559.

Schwartz, G.J. and Diller, K.R. (1983) Analysis of the water permeability of human granulocytes at subzero temperatures in the presence of extracellular ice. *ASME J. Biomech. Eng.,* **105**, 360–366.

Smith, D.J., Schulte, M. and Bischof, J.C. (1998) The effect of dimethylsulfoxide on the water transport response of rat hepatocytes during freezing. *ASME J. Biomech. Eng.*, **120**, 549–558.

Spallanzani, L. (1776) Osservation e spezien interno ai vermicelli spermatici dell'uomo e degli animali. In Opusculi di Fisica Animale e Vegetabile, Opusculo II. Modena, Italy (cited in Brotherton, 1990).

Steponkus, P.L. (1984) Role of the plasma membrane in freezing injury and cold acclimation. *Annu. Rev. Plant Physiol.*, **35**, 543–584.

Storey, B.T., Noiles, E.E. and Thompson, K.A. (1998) Comparison of glycerol, other polyols, trehalose, and raffinose to provide a defined cryoprotective medium for mouse sperm cryopreservation. *Cryobiology*, **37**, 46–58.

Toner, M. (1993) Nucleation of ice crystals in biological cells. In Steponkus, P.L. (ed.), *Advances in Low Temperature Biology.* JAI Press, London, vol. **2**, pp. 1–52.

Verkman, A.S., Van Hoek, A.N., Ma, T. *et al*. (1996) Water transport across mammalian cell membranes. *Am. J. Physiol. Cell Physiol.*, **39**, C12–C30.

Watson, P.F. (1981) The effects of cold shock on sperm cell membranes. In Morris, G.J. and Clarke, A. (eds), *Effects of Low Temperature on Biological Membranes*. Academic Press, London, pp. 189–218.

Watson, P.F. (1995) Recent developments and concepts in the cryopreservation of spermatozoa and the assessment of their post-thawing function. *Reprod. Fertil. Dev.*, **7**, 871–891.

Weidel, L. and Prins, G.S. (1987) Cryosurvival of human spermatozoa frozen in eight different buffer systems. *J. Androl.*, **8**, 41–47.

World Health Organization (1999) WHO Laboratory Manual for the Examination of Human Semen and Sperm–Cervical Mucus Interaction. 4th edn. Cambridge University Press, Cambridge.

Received on November 8, 1999; accepted on February 10, 2000